PNAS
www.pnas.org

Supplementary Information for

POPOVICH, encoding a C2H2-zinc finger transcription factor, plays a central role in the development of a key innovation, floral nectar spurs, in *Aquilegia*

Evangeline S. Ballerini, Ya Min, Molly B. Edwards, Elena M. Kramer, and Scott A. Hodges

Corresponding Evangeline S. Ballerini and Scott A. Hodges.
E-mail: ballerini@csus.edu, hodges@lifesci.ucsb.edu

This PDF file includes:

Figs. S1 to S9
Tables S1 to S4
Legend for Dataset S1
SI References

Other supplementary materials for this manuscript include the following:

Dataset S1

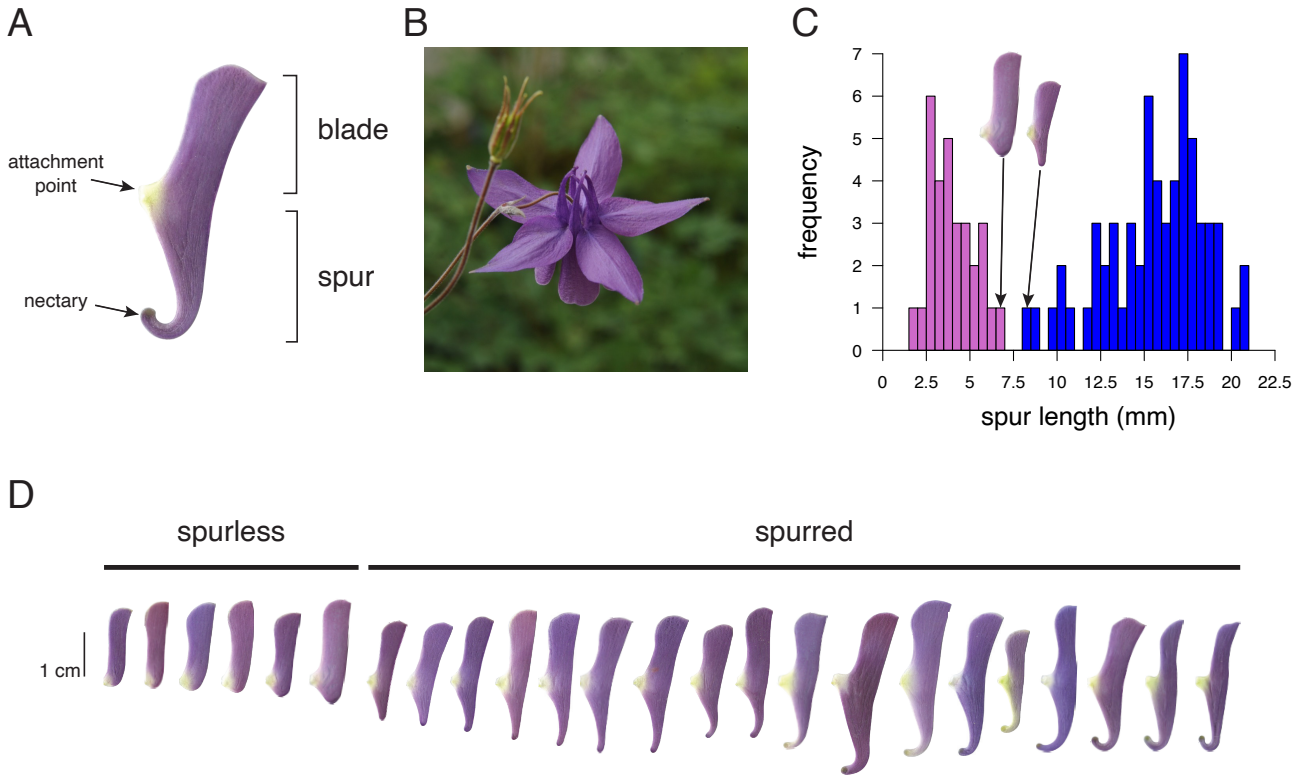

Fig. S1. ***Aquilegia* petal morphology and variation in the *A. sibirica* x *A. ecalcarata* F_1 and F_2 generations.** **A.** An example *Aquilegia* petal demonstrating the blade, spur, nectary, and attachment point. **B.** An *A. sibirica* x *A. ecalcarata* F_1 flower demonstrating spur morphology. **C.** Histogram of average spur length in 92 F_2 individuals showing a bimodal distribution and a break in the histogram between spurless individuals (lavender) and spurred individuals (blue). Measurements were made along the proximal edge from the attachment point to the nectary using ImageJ on all of the petals from two flowers per plant. Example petals are to scale. **D.** Examples of F_2 petals scored as spurless or spurred. Petals were folded longitudinally and scanned on a flat bed scanner. Petal attachment points are on the left. In addition to differences in length, spurless petals with a pocket were distinguishable from short spurred petals by the shape of the outgrowth: spurless petals had a rounded pocket whereas short spurred petals formed a more narrow point.

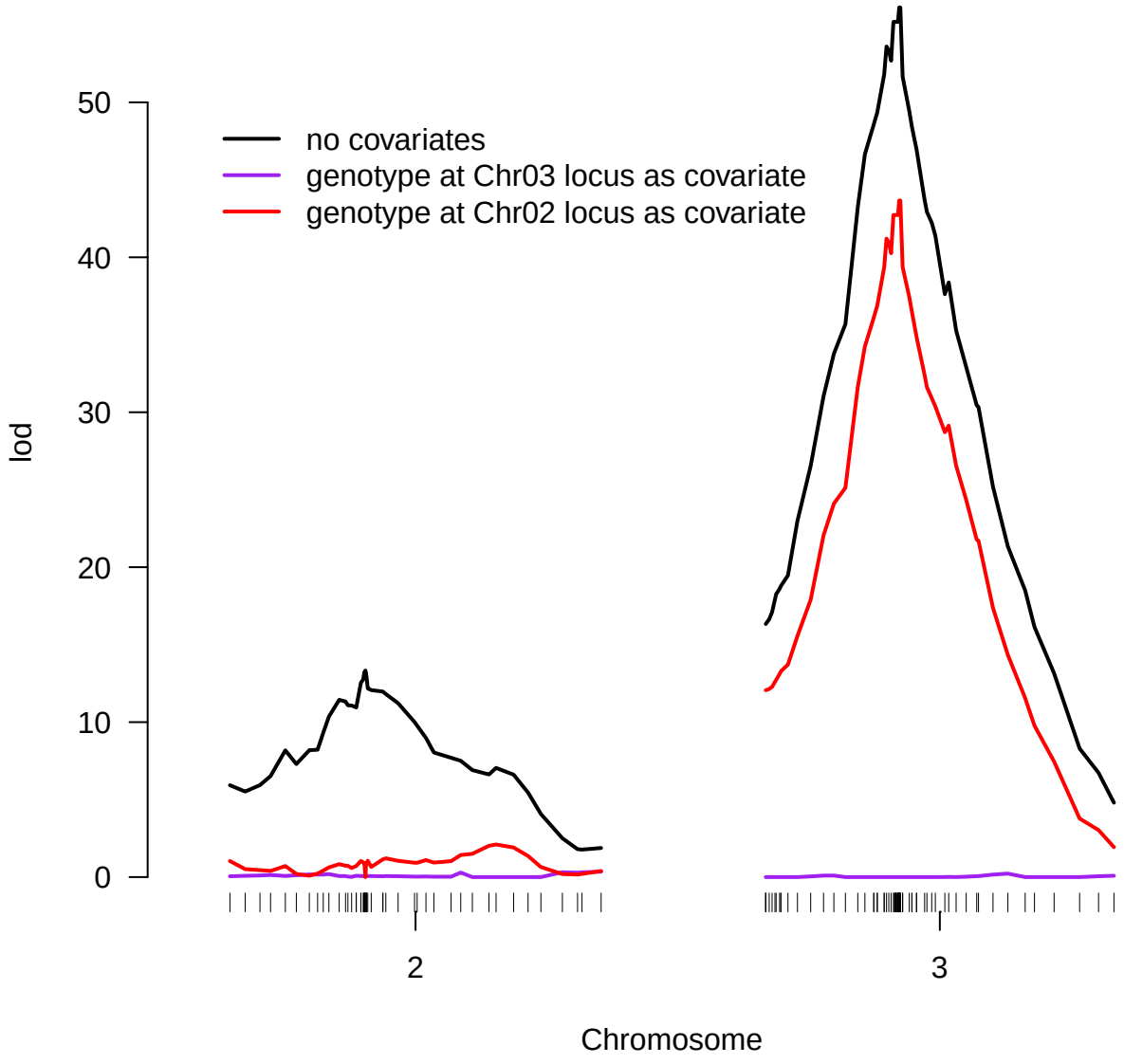

Fig. S2. Association between genotype and phenotype on chromosome 2 is caused by a deleterious interaction with genotypes on chromosome 3. The scanone LOD score for the spur phenotype with no covariates considered (black) versus the LOD score when considering either the genotype at the chromosome 2 LOD peak as a covariate (red) or the genotype at the chromosome 3 LOD peak as a covariate (purple) indicates that the peak on 2 is related to the genotype at chromosome 3

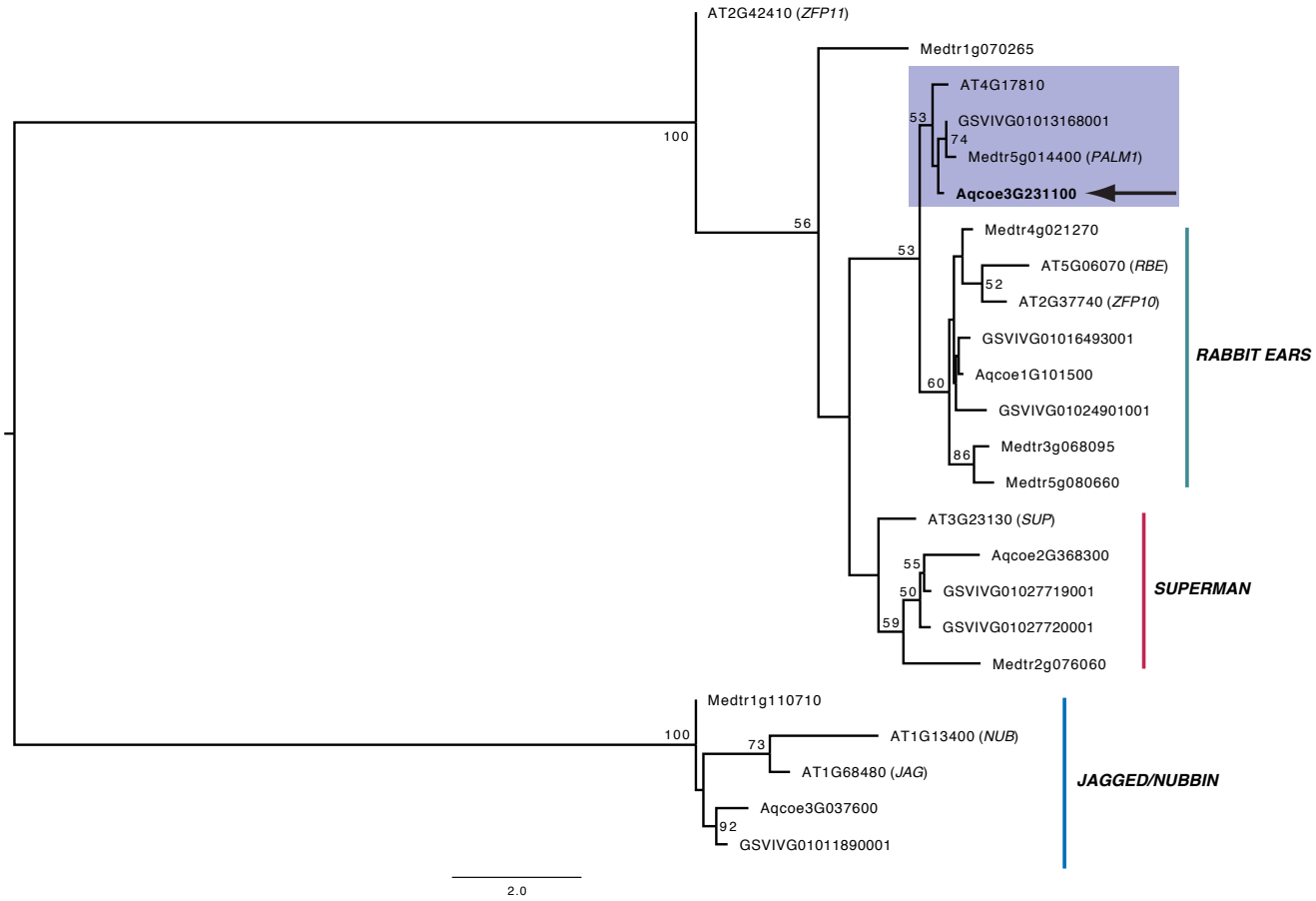

Fig. S3. Gene tree of the C2H2-zinc finger TF clade containing Aqcoe3G231100. Aqcoe3G23110 (arrow) is in a clade with *Medicago truncatula PALM1*. This clade is closely related to clades containing the Arabidopsis genes *RABBIT EARS* (*RBE*) and *SUPERMAN* (*SUP*). A clade containing the Arabidopsis genes *JAGGED* (*JAG*) and *NUBBIN* (*NUB*) was used to root the tree. The tree was generated using RAxML on aligned protein sequences. Bootstrap support of nodes greater than 50 are indicated. BLAST hits from the *Aquilegia*, (Aqcoe-), Arabidopsis (AT-), *M. truncatula* (Medtr-) and *Vitis vinifera* (GSVIVG-) genomes were included.

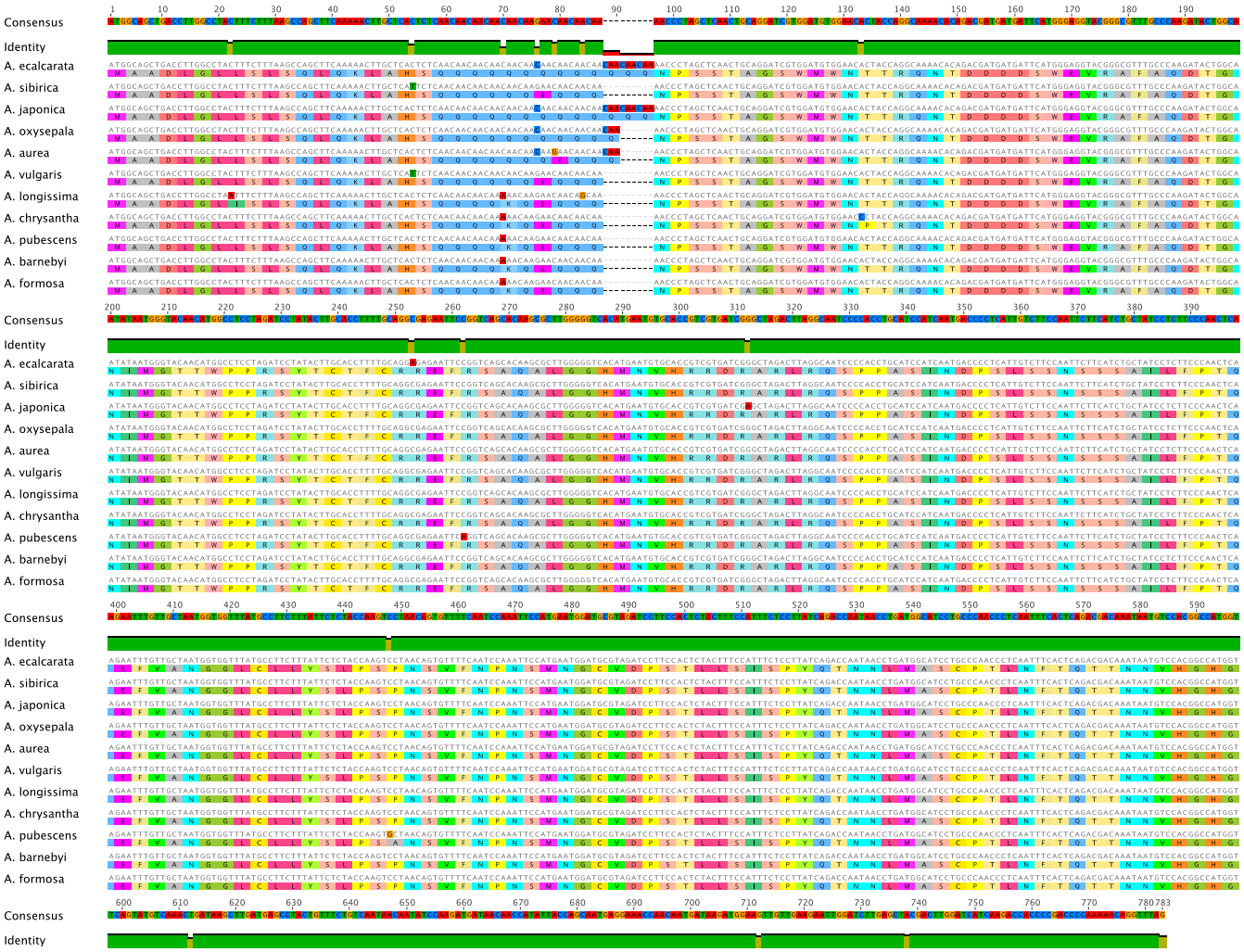

Fig. S4. Aqcoe3G231100 sequence alignment. The coding sequence and amino acid translation alignment of Aqcoe3G231100 from the cross parents and nine additional *Aquilegia* species from Eurasia and North America showing high conservation. *A. ecalcarata* is spurless while all other species included have spurs.

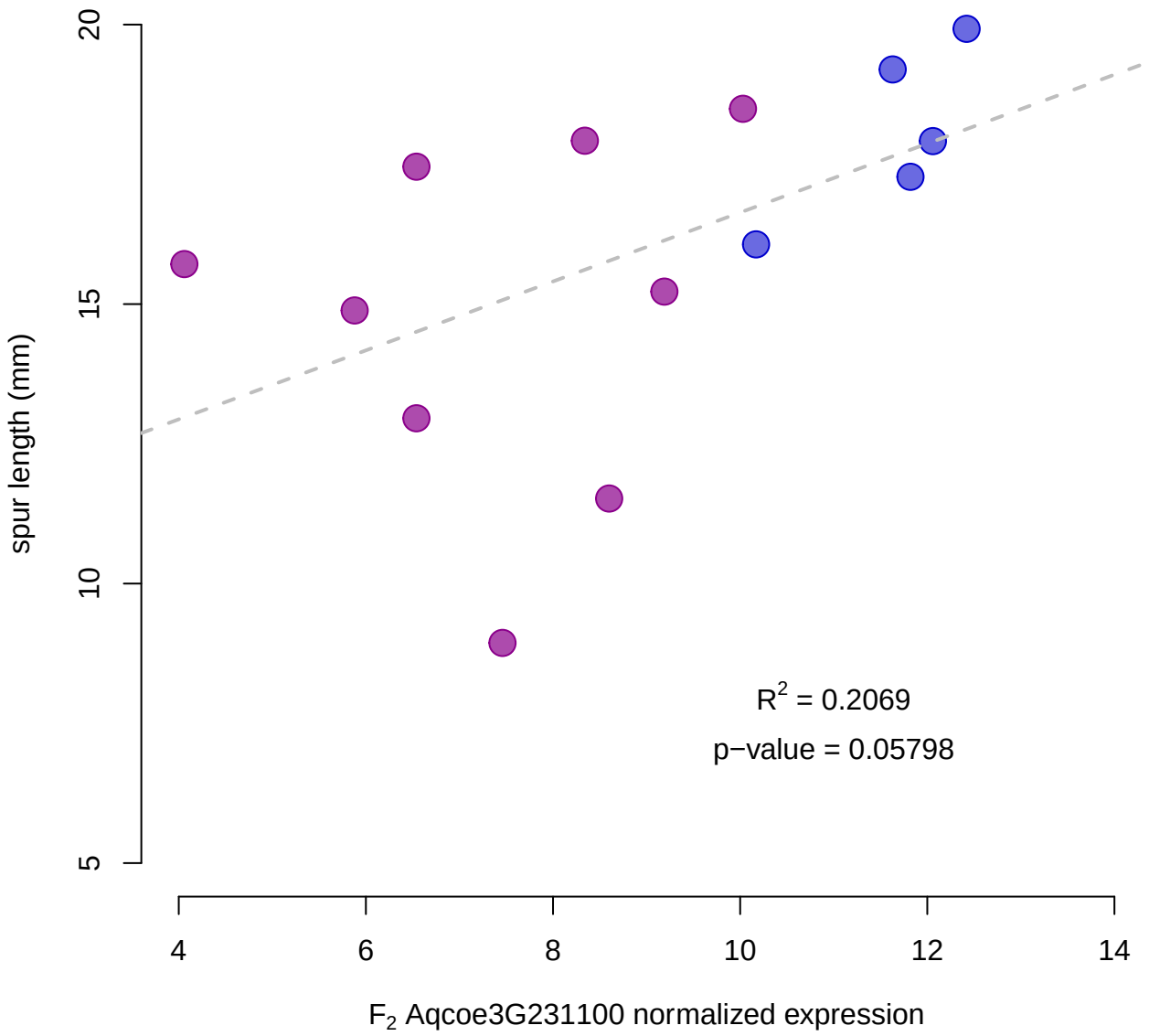

Fig. S5. The relationship between Aqcoe3G231100 expression and spur length (mm) in spurred F_2 individuals. The expression level of Aqcoe3G231100 is not significantly correlated with spur length in the spurred F_2 individuals examined (R^2 = 0.21, p = 0.058, n=14). Individuals heterozygous at Aqcoe3G231100 (ES, n=9) are in magenta, homozygous *A. sibirica* individuals (SS, n=5) are in blue. While RNAseq was conducted on 10 ES individuals, there was no scan for one individual and thus there are only 9 length measurements.

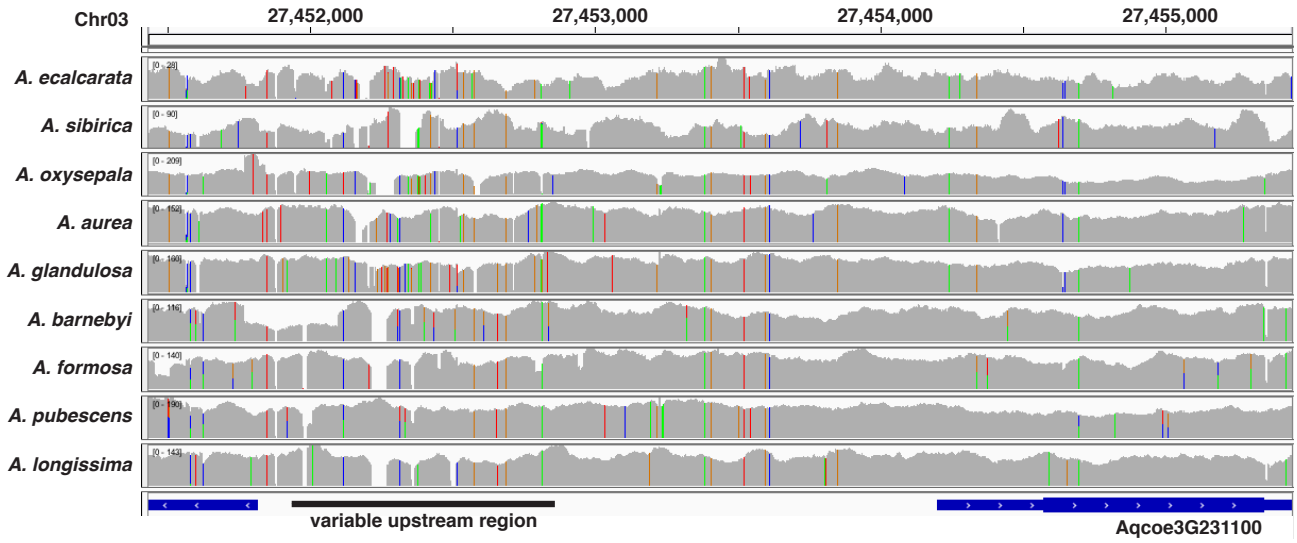

Fig. S6. **Upstream sequence variation at Aqcoe3G231100.** Sequence depth from an *A. ecalcarata* individual related to the parent and the *A. sibirica* parent along with sequence from seven additional *Aquilegia* individuals from various Eurasian and North American taxa as captured using the Integrative Genomics Viewer (1). *A. ecalcarata* is spurless while all other species included have spurs. Grey indicates that sequence reads are the same as the *Aquilegia* v3.1 reference genome while colored reads indicate single nucleotide variants and gaps in coverage indicate deletions. While there are very few unique variants in the ∼1 kb just upstream of Aqcoe3G231100 in *A. ecalcarata*, the region ∼1.5-2 kb upstream is highly variable across the genus.

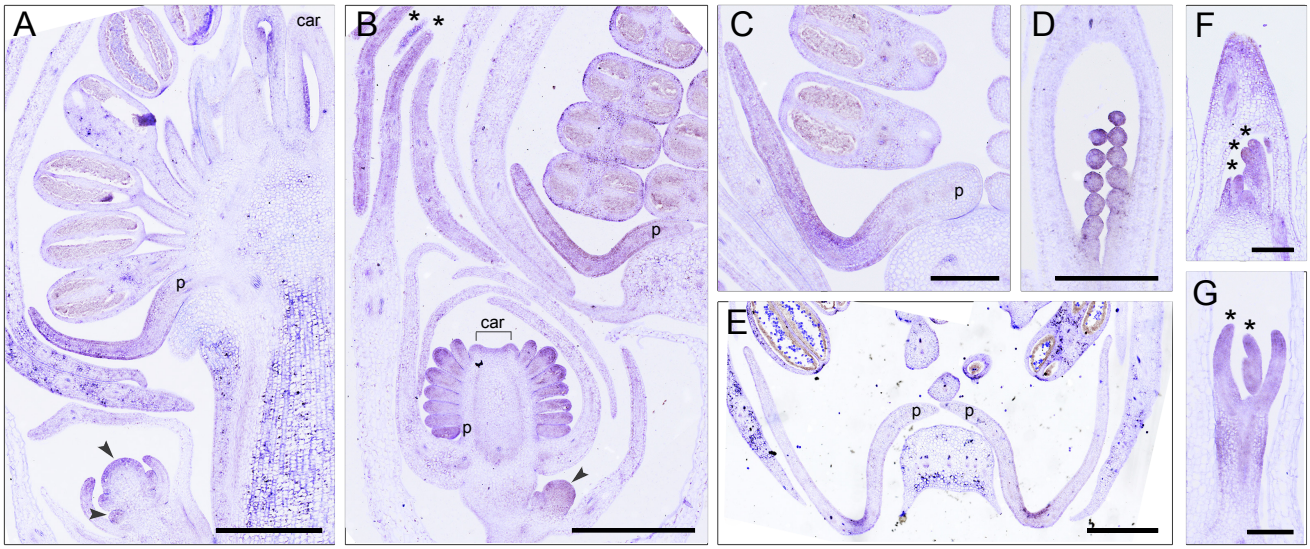

Fig. S7. Spatial expression of Aqcoe3G231100 during floral and vegetative development in *A. coerulea* 'Origami'. **A.** This panel shows meristems at three separate phases of development. In the lowermost left (bottom arrowhead), a stage 1 pre-floral meristem (all stages reference Ballerini and Kramer 2011) shows constitutive Aqcoe3G23110 expression, while immediately adjacent to the right is a stage 4 floral meristem with similarly broad expression (upper arrowhead). In the large stage 9 meristem (top), Aqcoe3G231100 is detected throughout the petal and in the placental tissue of the carpel (car). **B.** Again, this panel shows several different stages of floral meristems. At the bottom center (arrowhead), a stage 2-3 floral meristem shows expression throughout. Adjacent to the left, a stage 7 floral meristem has Aqcoe3G23110 expression in all early petals, stamens, staminodes and carpels (car). In the upper right, a stage 9 floral meristem shows strong expression throughout the petal. **C.** An early stage 10 floral meristem with Aqcoe3G231100 expression detected in most of the petal but starting to show signs of concentration in the initiating spur cup. **D.** A stage 11 carpel with expression in initiating ovules. **E.** Stage 10-11 floral meristem with concentrated Aqcoe3G231100 expression in the developing spur cup. **F-G.** Expression of Aqcoe3G231100 in developing vegetative leaflets (asterisks). Scale bars: **A**, **B**, and **E** = 500 μm; **C**, **D**, **F**, and **G** = 200 μm. Arrows = early floral meristems, asterisk = leaves, p = petals, car = carpels.

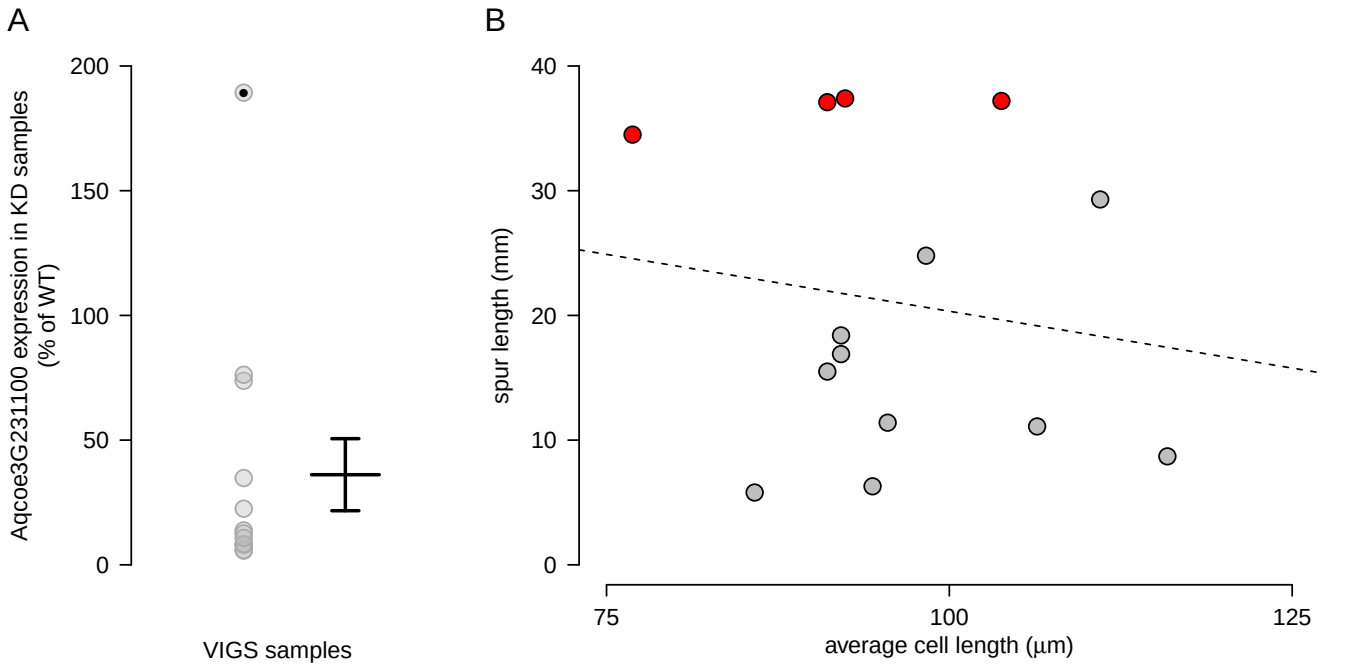

Fig. S8. **Aqcoe3G231100 expression and cell lengths in *A. coerulea* 'Origami' VIGS KD vs. WT. A.** Percent expression of Aqcoe3G231100 in VIGS KD petals relative to paired WT petals (n=13, mean=36.1%, +/- SE presented on the right). We suspect that the KD and WT samples may have been mistakenly switched during tissue collection, RNA isolation, or cDNA preparation in the outlier sample (black dot). **B.** Spur length (mm) plotted against average cell length (μm) in several WT (red) and KD (grey) spurs showing no significant correlation between cell length and spur length (R^2 = 0.02, p = 0.60).

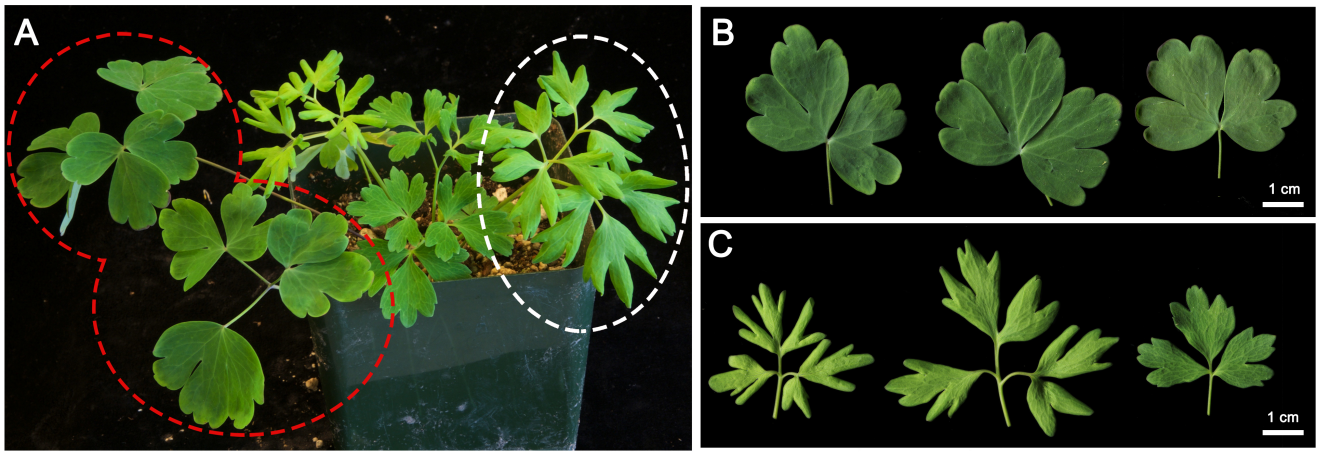

Fig. S9. **Leaf phenotype of Aqcoe3G231100 VIGS knock-down in *A. coerulea* 'Origami'.** **A.** Leaves on the same plant with examples of wild type leaves that began developing prior to VIGS treatment (circled in red) and those exhibiting a phenotype with more highly dissected leaflets and lanceolate laminae that developed following VIGS treatment (circled in white). **B-C.** Scans of individual leaflets from separate leaves. **B.** Wild type leaflets. **C.** VIGS leaflets exhibiting various degrees of morphological perturbation.

Table S1. Genotype counts at LOD peaks on chromosome 2 and chromosome 3 indicative of a deleterious interaction between *A. ecalcarata* and *A. sibirica* alleles.

		Chr03 QTL			
		EE	ES	SS	NA
Chr02 "QTL"	EE	25	0	0	0
	ES	46	95	1	1
	SS	12	51	55	0
	NA	0	0	0	0

Table S2. Counts of spurred and spurless F_2 individuals by genotype at the LOD peak on chromosome 3

	Genotype at Chr03 QTL			
	EE	ES	SS	NA
spurred	8	141	55	1
spurless	71	0	0	0
not phenotyped	4	5	1	0

Table S3. Dunnett modified Tukey-Kramer test showing a significant difference in mean expression of Aqcoe3G231100 by each genotype in $\mathbf{F_2}$ plants, confidence intervals (CI, $\alpha = 0.05$) do not overlap with 0

Genotype comparison	Difference in mean	Lower CI	Upper CI
EE-SE	5.32	3.05	7.60
SE-SS	3.42	0.13	6.71
EE-SS	8.74	6.68	10.81

Table S4. Cross reference of *Aquilegia* floral stages as used for describing *in situ* hybridization (from (2)), RNAseq (from (3)), qRT-PCR, and petal phase (from (4))

Description	Floral developmental stage	RNAseq stage	*A. coerulea* 'Origami' spur length (mm)	Petal phase
Petal primordia arise	4	NA	NA	I
Stamen primordia begin arising	5	NA	NA	I
Sepals enclose bud, stamen primordia continue appearing	6	NA	NA	I
Carpels initiate, staminodia distinguishable, first whorl of stamens becoming stalked at base	7	NA	NA	I
Petal primordia begin to differentiate, first whorl of stamens begin to differentiate locules, folded carpels remain open	8	NA	NA	I
Petals continue to differentiate and elongate to same length as first whorl stamens, all stamens differentiating, staminodia still filamentous, carpels elongated to same height as innermost stamens but remain open, staminodia begin to flatten	9	1-2	NA	I
Spur formation initiates on petals, all organs elongating	10	3-5	∼0-8	I
Spur elongation continues, carpels close, stamens become apiculate	11	NA	∼8-40	II
Spurs and all floral organs reach final length	12	NA	∼40-45	II

SI Dataset S1 (gen.w.phen.csv)

The genotype and phenotype file used to conduct QTL mapping. A alleles correspond to the *A. sibirica* allele and B alleles correspond to the *A. ecalcarata* allele. The file is formatted as a .csvr file for reading into R/qtl.

References

1. JT Robinson, et al., Integrative genomics viewer. *Nat. Biotechnol.* **29**, 24–26 (2011).
2. ES Ballerini, EM Kramer, Environmental and molecular analysis of the floral transition in the lower eudicot *Aquilegia*. *EvoDevo* **2**, 1–20 (2011).
3. ES Ballerini, EM Kramer, SA Hodges, Comparative transcriptomics of early petal development across four diverse species of *Aquilegia* reveal few genes consistently associated with nectar spur development. *BMC Genomics* **20**, 668–23 (2019).
4. L Yant, S Collani, J Puzey, C Levy, EM Kramer, Molecular basis for three-dimensional elaboration of the *Aquilegia* petal spur. *Proceedings. Biol. Sci.* **282** (2015).